Crack Front Dynamics across a Single Heterogeneity

J. Chopin, A. Prevost, A. Boudaoud, and M. Adda-Bedia

Laboratoire de Physique Statistique, Ecole Normale Supérieure, UPMC Paris 06, Université Paris Diderot, CNRS, 24 rue Lhomond, 75005 Paris, France

We study the spatiotemporal dynamics of a crack front propagating at the interface between a rigid substrate and an elastomer. We first characterize the kinematics of the front when the substrate is homogeneous and find that the equation of motion is intrinsically nonlinear. We then pattern the substrate with a single defect. Steady profiles of the front are well described by a standard linear theory with nonlocal elasticity, except for large slopes of the front. In contrast, this theory seems to fail in dynamical situations, i.e., when the front relaxes to its steady shape, or when the front pinches off after detachment from a defect. More generally, these results may impact the current understanding of crack fronts in heterogeneous media.

Understanding the fundamental problem of how materials break or debond from a substrate is of great importance for a wide range of applications. It has been recognized that rupture processes are highly dependent on microstructures like impurities, voids, grain boundaries or fibers which can make the material either weaker or tougher [1]. Whereas many studies have considered averaged or macroscopic quantities such as the fracture energy, we focus here on the local properties of a front propagating in a disordered medium. In this context, a crack front can be modeled as a line having a nonlocal elasticity [2] with a noisy forcing (see, e.g., [3] for a review). This general approach has led to numerous theoretical and numerical results [4–6], but only a single setup [7,8] has enabled experimental studies which raised the issue of controlling the noise imposed by a heterogeneous material composition. Here we address this control, focusing on the scale of a single heterogoneity. Inspired by experiments on wetting contact lines [9–13] in which the heterogeneities are imposed through the patterning of the substrate, we designed a setup which has allowed us to investigate the motion of a crack front interacting with defects of tunable shape and size. Surprisingly, the fundamental question of how a crack front interacts with isolated defects has attracted little attention [14,15]. In this Letter, we characterize the kinematics of the crack front and then present results concerning the linear and nonlinear spatiotemporal response of the front when it crosses a single defect.

In the present experiments, a silicon elastomer block is peeled from a glass substrate in a beam cantilever configuration (Fig. 1). The crack front is defined as the frontier between bonded and debonded regions. The glass substrate can be made chemically heterogeneous in order to spatially modulate the fracture energy, Γ, or the toughness, K_c, of the interface. It is fabricated using soft lithography techniques. A primer and a photoresist (Ti-Prime and AZ5214, MicroChems) are successively spin coated on the substrate

which is then exposed to UV light through a patterned mask (Selba, CH). Exposed regions are dissolved in a solvent (MIF780, MicroChems) while protected ones remain on the substrate. A chromium layer of typical thickness 2 nm is then deposited using a Joule effect evaporator. The underlying resin is dissolved in an acetone bath sonicated for 15 s. A last step consists in cleaning the substrate with a Piranha solution ($H_2SO_4 : H_2O_2$, 2:1) for 1 h, rinsing it with deionized water and drying it with N_2. All steps are undertaken in a clean room environment. The defect consists of a glass strip surrounded by a layer of chromium [Fig. 1(b)]. Its width ranges from 10 to 10^3 μm while its length is at least 4 times larger than its width.

The elastomer is a crosslinked PolyDiMethylSiloxane (PDMS Sylgard184, Dow Corning) with a Young's modulus $E \simeq 2$ MPa. It is prepared by mixing an oligomer together with a silicon oil. The mixture is centrifugated, degased for 2 h under mild vacuum and poured in a mold covered with a clean glass slide. It is cured in an oven at
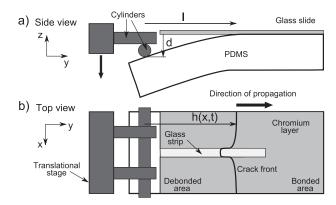

FIG. 1. Sketch of the experiment. (a) Side view. A silicon elastomer block is peeled from a patterned glass substrate by means of a translation stage imposing a deflection, d. (b) Top view. The substrate can be made chemically heterogeneous. Here, a glass strip of width $2a$ is surrounded by chromium.
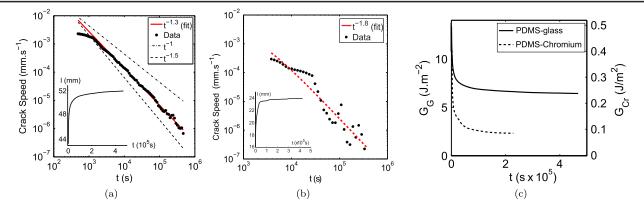
FIG. 2 (color online).   Creep tests for homogeneous PDMS-glass and PDMS-chromium interfaces. At $t = 0$ s, a deflection of 7 mm is applied for the glass interface and 0.180 mm for the chromium one. (a) and (b) Crack front velocities versus time. Insets: position of the crack l versus time (insets). For the glass interface (a), the velocity exhibits a well-defined power-law tail of the form $t^{-1.3}$. In dashed lines are shown power-law curves t^{-1} and $t^{-1.5}$ as a guide for the eyes. For the chromium interface (b), a power-law $t^{-1.8}$ is shown as a guide for the eye. (c) Energy release rates G versus time (left y axis for glass and right y axis for chromium). Note the difference in scale between the two y axes.

75° C for at least 2 h. The resulting crosslinked PDMS block is then demoulded without removing the glass slide from it, so that the interface remains clean. Blocks are 10 mm thick, 76 mm long, and either 22 or 72 mm wide. To enhance optical contrast between bonded and debonded regions, an additional 0.5 mm thick layer of a black crosslinked PDMS (Sylgard170, Dow Corning) is spread uniformly on the uncovered side of the block. The protective glass slide is removed and the patterned one is laid without pressure on the elastomer with a slight angle that is decreased progressively enabling an adhesive front to propagate slowly along the whole surface. Using this protocol, no air bubble nor dust is trapped (this has been checked by inspection with a microscope). The sample is left with the PDMS downside for at least 12 h prior to peeling. A longer waiting time does not change the results.

The glass substrate is clamped on an aluminum frame. A deflection d is applied to the edge of the elastomer using two cylinders rigidly attached to a translation stage driven by a stepper motor (NanoPZ, Newport) (Fig. 1). An additional cylinder is glued to the elastomer using a crosslinker-liquid PDMS mixture, thus providing two cross-cylinder contacts with reduced friction and without induced tension. The sample is lit up from above with a LED ring mounted on a binocular and pictures (3872 $\times$ 2576 px^2) are taken with a digital camera (Nikon, D300). The crack front appears as a bright line (see inset of Fig. 3) and its position $h(x, t)$ (see Fig. 1) is determined using a home made algorithm based on detecting pixels of highest intensity. Knowing $h(x, t)$, one can define the mean position of the front $l(t) = \langle h(x, t) \rangle_x$ as the spatial average of h along the transverse direction x. Depending on the optics used, binocular (MZ16,Leica) or macro objective (Nikon), 1 pixel corresponds to either 2 μm or 15 μm, respectively.

Before investigating the interaction of the front with defects, we characterized our system by measuring the

fracture properties of PDMS-glass and PDMS-chromium interfaces. We performed creep tests using homogeneous substrates, by imposing a constant deflection (reached in 50 s) and recording the evolution of $h(x, t)$ over longer times. Figure 2 shows typical results for PDMS-glass and PDMS-Chrome interfaces. The crack appears to reach asymptotically an equilibrium position l_{eq} with a mean velocity $v(t) = dl/dt$ which decreases with time. For the PDMS-glass interface, $v(t)$ is found to have a power-law dependence with an exponent -1.3 ± 0.05. For the PDMS-chromium interface, $v(t)$ has on average a power-law decrease, however, with superimposed fluctuations. The latter are presumably due to daily temperature variations or to small imperfections in the chromium layer.

Such observations can be rationalized _à la_ Maugis [16]. Let G be the energy release rate, i.e., the energy dissipated during fracture per unit of newly created fracture surface area. In our case, this energy is stored in the elastic bending of the cantilever, so that it is proportional to its bending
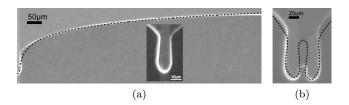

FIG. 3.   The steady profile of a crack front (appearing as the bright line) in the presence of a single or a double glass strip (lighter gray areas) of width $2a = 20$ μm. (a) The crack front has an infinite slope at the edge of the strip (nonlinear regime), but the tails are well fitted by Eq. (3) (dashed line). Inset: zoom on the tip of the front. (b) Interaction of the front with two parallel strips. The distance between the strips midlines is 30 μm. The predicted shape of the crack front position with two strips assuming a linear superposition of the solutions of Eq. (3) (dashed line) differs significantly from the real profile.

stiffness and to the curvature squared, $G(l) = 3/8Eh^3(d/l^2)^2$, where E is the Young's modulus and h the thickness of the elastomer. The time evolution of G is shown in Fig. 2(c) for two typical experiments with glass (G_G) and chromium (G_{Cr}) interfaces. At equilibrium ($v = 0$ and $l = l_{eq}$), the energy release rate $G(l_{eq})$ becomes equal to the fracture energy Γ, so that $\Gamma = 3/8Eh^3(d/l_{eq}^2)^2$. Measurements for different realizations yield Γ^G in the range 6–8 J·m^{-2} for PDMS glass and a much smaller value Γ^{Cr} in the range 0.08–0.2 J·m^{-2} for PDMS chromium. For both interfaces, the range of fracture energies is found to be rather large, but can be explained when considering the error made on the measure of l, of the order of 2 mm, and mainly due to the front small curvature. Since G depends strongly on l, any error on l will thus lead to errors on G of about 20% and 40% for the glass and chromium interfaces, respectively. Out of equilibrium ($v > 0$), the following equation of motion has been proposed [16]:

$$v = c\left(\frac{G}{\Gamma} - 1\right)^{1/n}, \quad (1)$$

where c is a velocity characterizing dissipative processes and n is the stretch exponent. Close to equilibrium and using the values of G and Γ given above, we expand Eq. (1) as $v \simeq 4^{1/n}c(1 - l/l_{eq})^{1/n}$, whose solution scales as $v \sim t^{-1/(1-n)}$. For a PDMS-glass interface, the stretch exponent $n = 0.25 \pm 0.01$ is in the same range as found in previous studies [16–18], with $c \sim 50$ μm·s^{-1}. If we force the power-law fit for PDMS chromium, we find similar values, $n \simeq 0.4$ and $c \sim 20$ μm·s^{-1}. Note that this behavior clearly differs from the exponential relaxation expected in the case of a linear equation of motion ($n = 1$).

We now operate at velocities much smaller than c, so that the energy release rate is close to the fracture energy ($G \simeq \Gamma$). We note that the following experiments have a typical duration of 2 h smaller than the daily fluctuations observed for chromium. We begin by considering the profile of the crack front when it propagates in steady state with a heterogeneous interface. Using a glass strip of width $2a = 20$ μm surrounded by chromium (Fig. 1), we can compare our experimental results with theoretical predictions. Adhesion contrast between PDMS glass and PDMS chromium interfaces is so high that the crack front remains pinned back on the chromium strip (Fig. 3). As a result, the PDMS block is highly deformed almost exhibiting infinite slopes at both edges [Fig. 3(a)]. We argue that, even in a regime of high toughness contrast ($\frac{\delta K_c}{K_c^{Cr}} > 1$), a linear theory might help predicting the shape of the front. The linear perturbation of the height $\delta h(x) = h(x) - l$, with $l \equiv \langle h(x) \rangle$, is governed by [2]:

$$\frac{\delta K_c}{K_c^{Cr}} = -\frac{\delta h(x)}{2l} + \frac{1}{2\pi}\text{PV}\int \frac{\delta h(x') - \delta h(x)}{(x' - x)^2} dx', \quad (2)$$

where PV is the principal value of the integral, $\delta K_c = (K_c^G - K_c^{Cr})$ is the toughness contrast and K_c^{Cr} (K_c^G) is the

toughness of a PDMS-chromium interface (PDMS-glass interface). Recall that the toughness K_c is related to the fracture energy through Irwin's formula $\Gamma = K_c^2/2E$. When $|\delta h| \ll l$, the solution of Eq. (2) is

$$\frac{1}{H}\delta h(x) = \left(1 + \frac{x}{a}\right)\ln\left|1 + \frac{x}{a}\right| + \left(1 - \frac{x}{a}\right)\ln\left|1 - \frac{x}{a}\right|, \quad (3)$$

where $H = 2a\pi^{-1}\delta K_c/K_c^{Cr}$ is a characteristic length scale. With $2a = 20$ μm, Eq. (3) provides a reasonable fit of the tails of the profile giving $H = 19$ μm. However, the resulting value of $\delta K_c/K_c^{Cr} \simeq 3$ is smaller than the one computed from the measured fracture energies $\delta K_c/K_c^{Cr} = \sqrt{\Gamma^G/\Gamma^{Cr}} - 1$ in the range 5–9. If we measure the size of the tip [Fig. 3(a), inset] defined as $\delta h(a) = 2\ln 2H$, we find $\delta h(a) \simeq 80$ μm yielding $\delta K_c/K_c^{Cr} \simeq 9$, in better agreement with the ratio of fracture energies. With two strips, the linear superposition of the solution does not allow us to recover the shape of the whole front [Fig. 3(b)]. As a partial conclusion for steady fronts, a linear theory provides a good description of the tails of the front whereas nonlinear effects seem to become important when the slope is $\gtrsim 1$.

We now move on to the dynamics of the front just after it leaves the glass strip (see Fig. 1), investigating the relaxation of the front shape towards a straight line in the homogeneous chromium interface (Fig. 4). The velocity
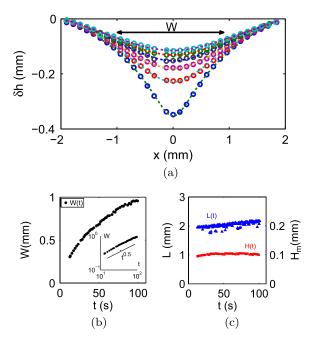

FIG. 4 (color online).   (a) Relaxation of the crack front during the first 100 s following its detachment from the glass strip. Experimental data ($\bigcirc$) are fitted by Eq. (4) (dashed line). For clarity, fronts are shown at intervals of 20 s. (b) and (c) Fitting parameters W ($\bullet$), H ($\blacksquare$), and L ($\blacktriangle$) of Eq. (4) as a function of time. H_m and $L = 2.2$ are roughly constant whereas W increases nonlinearly with time. Inset: Log-Log plot of W versus t.

at the center of the front ($x = 0$) is about 2 μm $\cdot$ s^{-1} and is much faster than the tail velocity which is about 0.3 μm $\cdot$ s^{-1} at $|x| \sim 2$ mm. The front spreads as its typical width $W(t)$ increases with time. This phenomenology is reminiscent of the dynamics of a wetting contact line just after it detaches from a defect [11]. Here, Eqs. (1) and (2) determine completely the dynamics of the front. When Eq. (1) can be linearized around a constant velocity of the front, the dynamical equation is exactly the same as in wetting [11] and its solution takes the form

$$\delta h(x, t > 0) = H_m \ln\frac{x^2 + W(t)^2}{L^2}, \qquad (4)$$

where H_m is the typical front height and L a large scale cutoff. We used this equation to fit the shape of the front (Fig. 4). In the case of wetting H_m and L are constant, while $W = ut$ where u is a characteristic velocity of waves along the front. Here H_m and L are indeed constant, but surprisingly, W is found to increase nonlinearly with time ($\sim t^{1/2}$). This discrepancy might be ascribed to the intrinsic nonlinear nature of the equation of motion (1), which cannot be linearized for small velocities.

Finally, we come back to the complex depinning event. Figure 5 (inset) shows the necking of the tip of the crack front just after the end of the strip (horizontal dashed line). This necking increases until the two parts of the front merge and leave an isolated contact area behind. This corresponds to the formation of a PDMS filament attached to the end of the glass strip. We measured the size ΔX of the neck as a function of $\Delta t = t_r - t$, where t is time and t_r the instant of merging, for various values of the width of the stri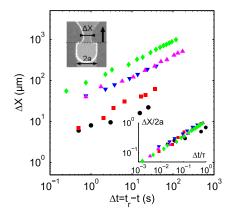p (Fig. 5). The whole data collapse on a master curve $\Delta X/2a = 1.17(\Delta t/\tau)^{0.47}$, where $\tau = 2a/v$ with v the mean velocity of the front evaluated from the tails.

In summary, we have designed an experiment where a crack front propagates in a controlled interface. In the presence of a defect, the steady profile of the crack front is captured by a standard linear nonlocal elastic equation except when the slopes are large (close to a defect). We identified sources of nonlinear behavior in the dynamics of the crack, during the spreading of a relaxing bump and pinch-off following the detachment from a defect. More fundamentally, the equation of motion appears to be intrinsically nonlinear and can lead to a complex dynamics as already reported in viscoelastic materials [19] and volume contraction induced fracturing in brittle materials [20,21]. These observations might have an impact on assumptions used in the modeling of the propagation of fronts in disordered media.

FIG. 5 (color online). Pinch-off from a strong defect. Evolution of the size of the neck ΔX as a function of $\Delta t = t_r - t$ for different widths $2a$ of the glass strip : 31 (●), 63 (□), 256 ($\triangledown$), 511 ($\triangle$), 1020 μm ($\diamond$). t is time and t_r the instant of topological change. Insets: picture of the crack front near the end of the glass strip; all data collapse on a master curve: $\Delta X/2a = 1.17(\Delta t/\tau)^{0.47}$, where $\tau = 2a/v$ with v the mean velocity of the front evaluated from the tails.

[1] B. Lawn, *Fracture of Brittle Solids* (Cambridge University Press, Cambridge, 1993), 2nd ed.
[2] H. Gao and J. R. Rice, J. Appl. Mech. **56**, 828 (1989).
[3] M. Kardar, Phys. Rep. **301**, 85 (1998).
[4] E. Bouchaud, J. Phys. Condens. Matter **9**, 4319 (1997).
[5] E. Katzav, M. Adda-Bedia, and D. Vandembroucq, Phys. Rev. E **73**, 035106 (2006).
[6] D. Bonamy, S. Santucci, and L. Ponson, Phys. Rev. Lett. **101**, 045501 (2008).
[7] J. Schmittbuhl and K. J. Måløy, Phys. Rev. Lett. **78**, 3888 (1997).
[8] S. Santucci, M. Grob, R. Toussaint, J. Schmittbuhl, A. Hansen, and K. J. Måløy, Europhys. Lett. **92**, 44001 (2010).
[9] T. Ondarçuhu and M. Veyssié, Nature (London) **352**, 418 (1991).
[10] G. Nadkarni and S. Garoff, Europhys. Lett. **20**, 523 (1992).
[11] J. A. Marsh and A. M. Cazabat, Phys. Rev. Lett. **71**, 2433 (1993).
[12] A. Paterson, M. Fermigier, P. Jenffer, and L. Limat, Phys. Rev. E **51**, 1291 (1995).
[13] S. Moulinet, C. Guthmann, and E. Rolley, Eur. Phys. J. E **8**, 437 (2002).
[14] T. Mower and A. Argon, Mech. Mater. **19**, 343 (1995).
[15] D. Dalmas, E. Barthel, and D. Vandembroucq, J. Mech. Phys. Solids **57**, 446 (2009).
[16] D. Maugis and M. Barquins, J. Phys. D **11**, 1989 (1978).
[17] E. H. Andrews and A. J. Kinloch, Proc. R. Soc. A **332**, 385 (1973).
[18] A. Crosby, K. Shull, H. Lakrout, and C. Creton, J. Appl. Phys. **88**, 2956 (2000).
[19] D. Maugis, J. Mater. Sci. **20**, 3041 (1985).
[20] B. Yakobson, Phys. Rev. Lett. **67**, 1590 (1991).
[21] A. Malthe-Sørenssen, B. Jamtveit, and P. Meakin, Phys. Rev. Lett. **96**, 245501 (2006).